Nat. Neurosci. **11,** 877–879 **(2008)**

Patches of face-selective cortex in the macaque frontal lobe

Doris Y Tsao, Nicole Schweers, Sebastian Moeller & Winrich A Freiwald

In the version of this supplementary file originally posted online, **Supplementary Figure 1** was incorrect. The error has been corrected in this file as of 23 July 2008.

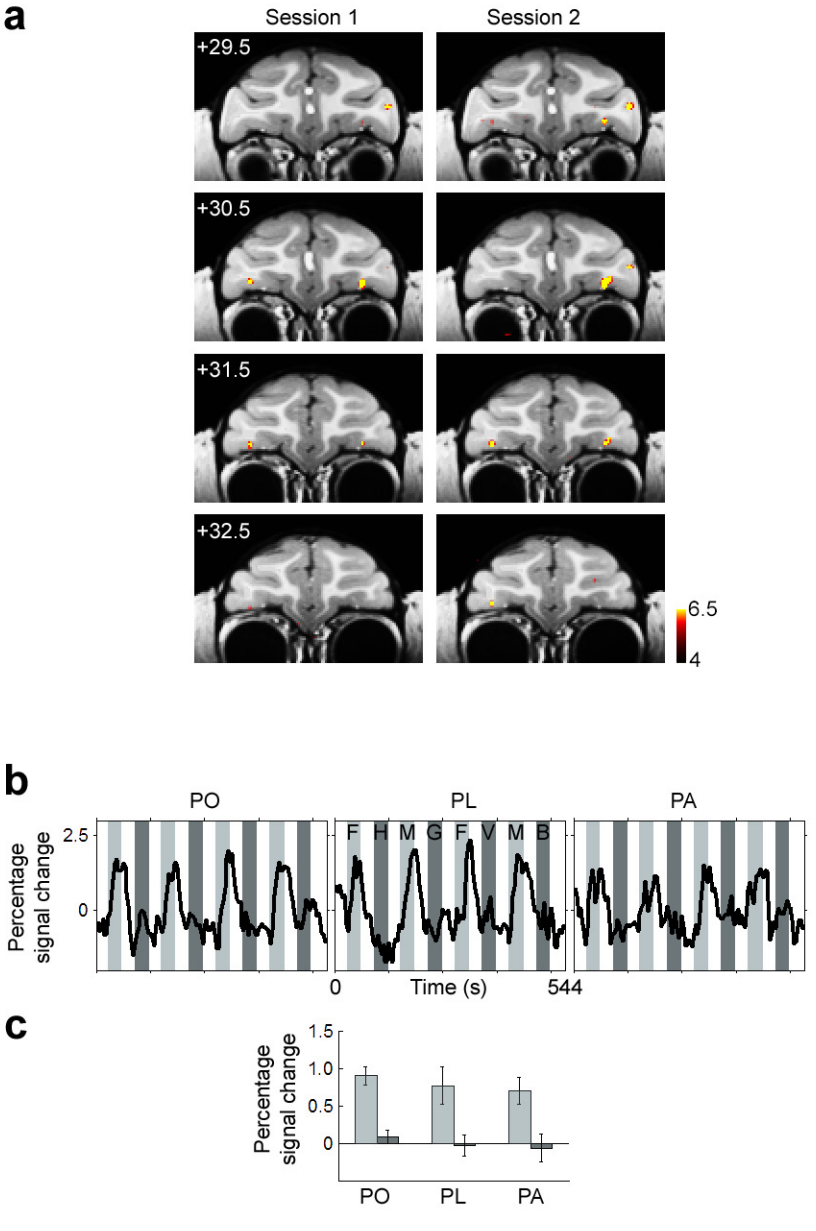
a
Session 1
Session 2
+29.5
+30.5
+31.5
+32.5
6.5
4
b
PO
PL
PA
Percentage signal change
2.5
0
F H M G F V M B
0
Time (s)
544
c
Percentage signal change
1.5
1.0
0.5
0
PO
PL
PA

Supplementary Fig. 1. Robustness of the macaque prefrontal face patches and response profiles extracted from full data set.

a) Prefrontal face patches in monkey M4 obtained in two independent scan sessions of 12 runs each.

b) Mean time courses from the three prefrontal face patches, averaged across monkeys and across hemispheres for patches that were bilateral. To generate the data shown here and in (c) below, all runs were used both to define ROI's and extract the time courses and activation values. Conventions as in Fig. 1d.

c) Bar graph showing % fMRI signal change to faces (light grey bars) and to non-face objects (dark grey bars).

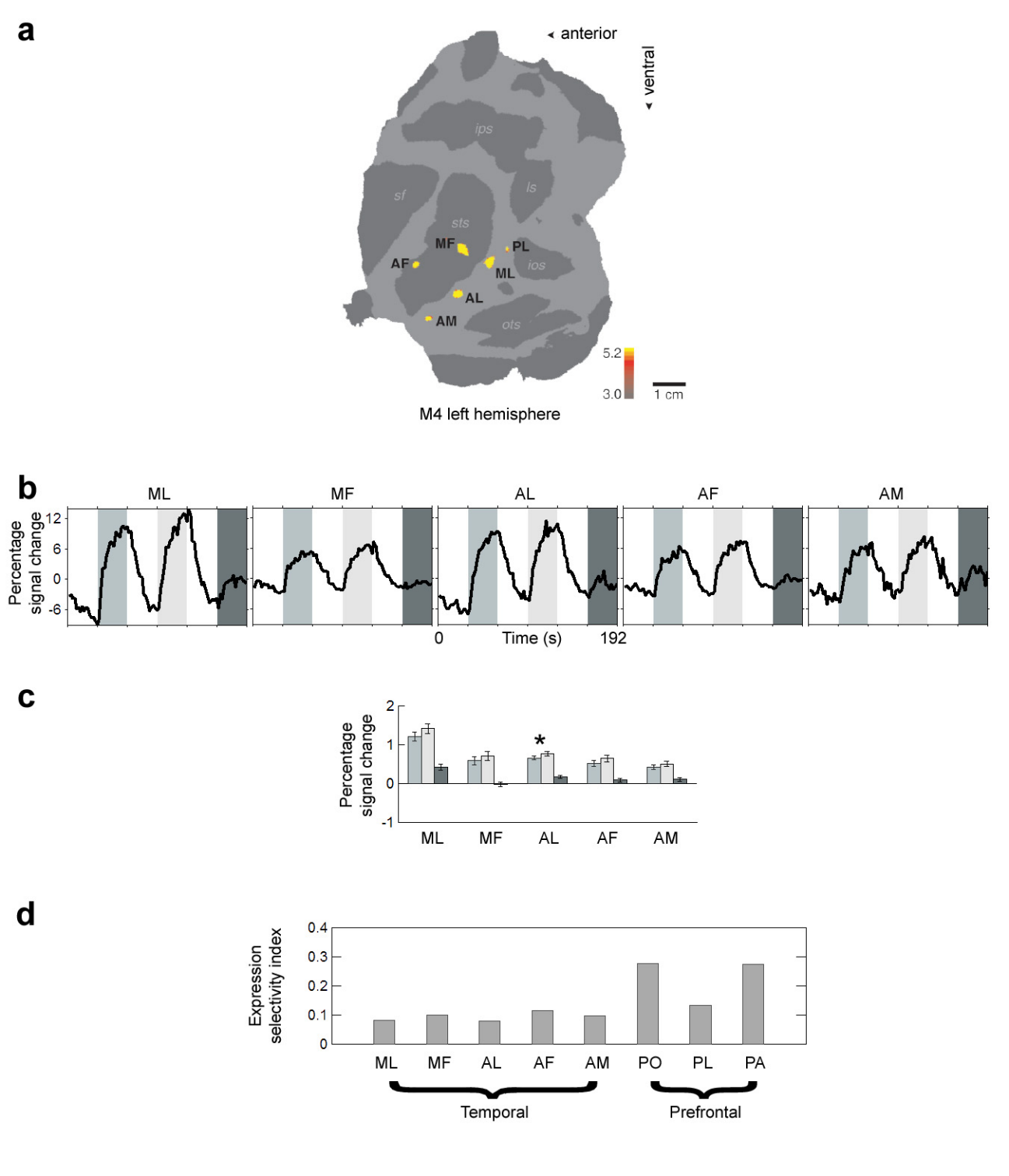
a
anterior
ventral
ips
sf
ls
sts
MF
PL
AF
ML
ios
AL
AM
ots
5.2
3.0
1 cm
M4 left hemisphere
b
ML
MF
AL
AF
AM
Percentage signal change
12
6
0
-6
0
Time (s)
192
c
Percentage signal change
2
1
0
-1
*
ML
MF
AL
AF
AM
d
Expression selectivity index
0.4
0.3
0.2
0.1
0
ML
MF
AL
AF
AM
PO
PL
PA
Temporal
Prefrontal

Supplementary Fig. 2. Sensitivity of temporal lobe face patches to facial expression. **a)** Six face-selective patches in the left hemisphere of monkey M4 (representative of most monkeys). The flattened cortical surface shows temporal lobe regions significantly more activated by faces than by other objects. Sulci are shown in dark grey. Area initials: posterior face patch (PL), middle face patch in the STS fundus (MF), middle face patch on the STS lip (ML), anterior face patch in the STS fundus (AF), anterior face patch on the STS lip (AL), and anterior face patch on the ventral surface of IT just lateral and anterior to the AMTS (AM). Anatomical labels: *sts:* superior temporal sulcus, *sf:* sylvian fissure, *ips:* intraparietal sulcus, *ls:* lunate sulcus, *ios:* inferior occipital sulcus, *ots:* occipitotemporal sulcus**.**

b) Average time course from ML, MF, AL, AF, and AM to neutral faces (medium grey), expressive faces (light grey), and non-face objects (dark grey). Data averaged across three monkeys (M1, M3, M4) and both hemispheres. The data were extracted from same experiment and using same methods as that shown in Fig. 2. The slice prescription did not include ML and MF for monkey M4, thus time courses for ML and MF were averaged only over monkeys M1 and M3. The posterior face patch (PL) was not included in the slice prescription for any of the monkeys.

c) Bar graph showing % fMRI signal change to neutral faces (medium grey), expressive faces (light grey), and non-face objects (dark grey). Data averaged across three monkeys (M1, M3, M4). Error bars indicate 95% confidence intervals. Results of t-test comparing activation to expressive versus neutral faces: ML, $p = 0.02$; MF, $p = 0.13$; AL, $p = 0.004$; AF, $p = 0.03$; AM, $p = 0.04$).

d) Bar graph of Expression Selectivity Index across temporal and prefrontal face patches. The Expression Selectivity Index, defined as $(\text{Response}_{\text{expressive}} - \text{Response}_{\text{neutral}}) / (\text{Response}_{\text{expressive}} + \text{Response}_{\text{neutral}})$, quantifies the degree of modulation of individual face patches by expression. The Expression Selectivity Indices of five temporal lobe face patches were much lower than those of PO and PA (Supplementary Fig. 2d).

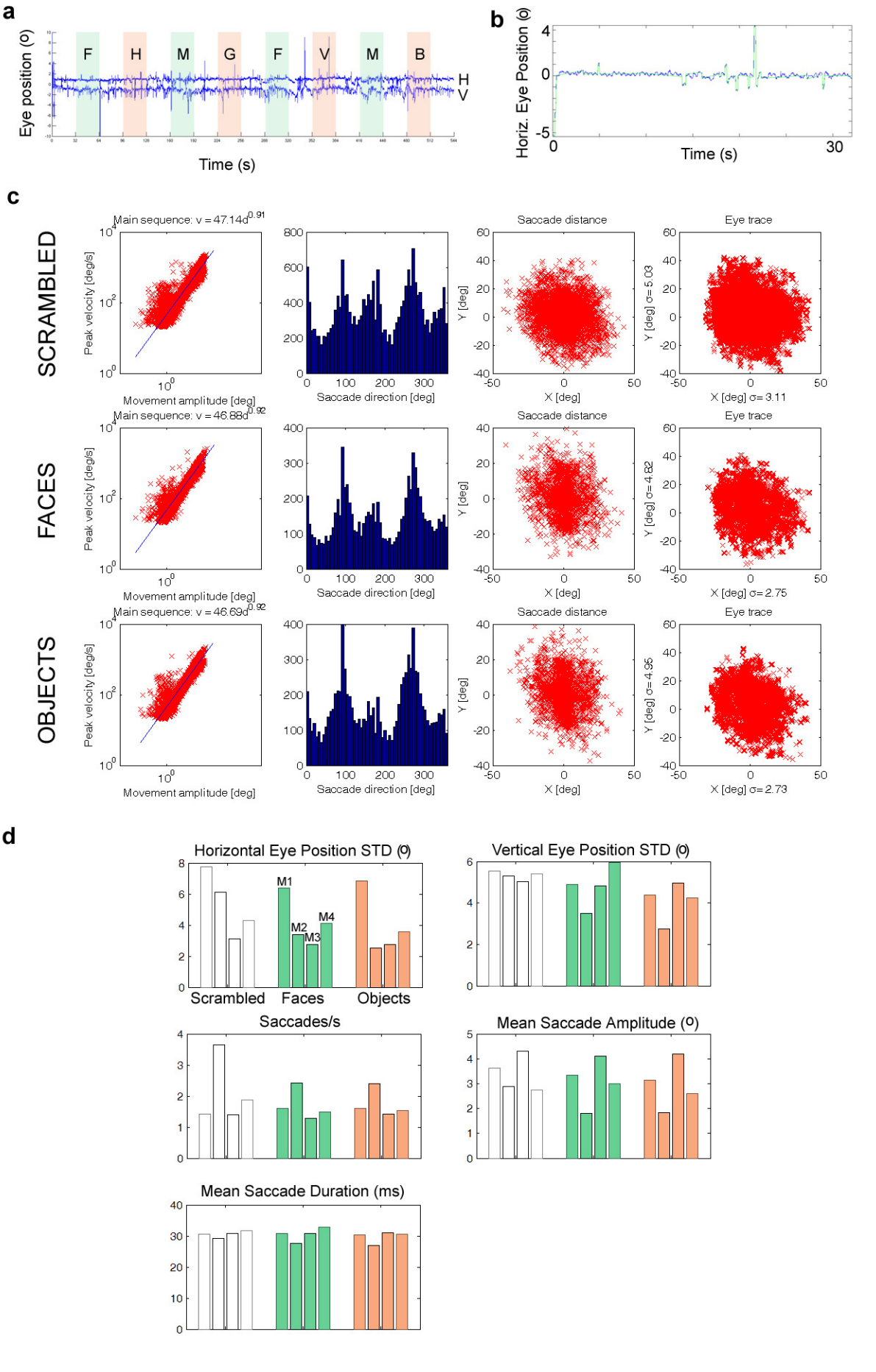
a
Eye position (º)
F
H
M
G
F
V
M
B
H
V
Time (s)
b
Horiz. Eye Position (º)
4
0
-5
0
Time (s)
30
c
SCRAMBLED
FACES
OBJECTS
Main sequence: v = 47.14d^0.91
Main sequence: v = 46.88d^0.92
Main sequence: v = 46.69d^0.92
Peak velocity [deg/s]
Movement amplitude [deg]
Saccade direction [deg]
Saccade distance
Y [deg]
X [deg]
Eye trace
Y [deg] σ= 5.03
X [deg] σ= 3.11
Y [deg] σ= 4.82
X [deg] σ= 2.75
Y [deg] σ= 4.96
X [deg] σ= 2.73
d
Horizontal Eye Position STD (º)
Vertical Eye Position STD (º)
M1
M2
M3
M4
Scrambled
Faces
Objects
Saccades/s
Mean Saccade Amplitude (º)
Mean Saccade Duration (ms)

Supplementary Fig. 3. Comparison of eye movements across different visual stimulus conditions.

a) An example eye movement trace (from monkey M3) showing the horizontal (H) and vertical (V) eye position during one run; eye blinks have been removed. Epoch identities are as in Fig. 1d (green epochs: faces, orange epochs: objects). For presentation purposes, the horizontal trace was shifted by 1° up, and the vertical trace by 1° down.

b) An example horizontal eye movement trace (blue trace, from monkey M3) together with fitted predictor (green trace) showing detected saccades, drifts, and periods of steady fixation (see Supplementary Methods for details).

c) Eye movement parameters across stimulus conditions for monkey M3 (other three monkeys showed similar results). Top row: Scrambled, middle row: Faces, bottom row: Objects. First column: plots of peak velocity versus movement amplitude; in all four monkeys and all three conditions, this plot approximated the "main sequence" relationship of v = 70d reported by [12]. Second column: saccade direction distributions; all four monkeys showed a preference for vertical and horizontal over other saccade directions. Third column: scatter plots of saccade displacement vectors. Fourth column: scatter plots of vertical (y) versus horizontal (x) eye positions.

c) Bar graphs showing the standard deviation of the horizontal and vertical eye positions, the saccade frequency, the mean saccade amplitude, and the mean saccade direction, computed separately for each monkey and each stimulus condition (scrambled patterns, faces, objects). For each monkey and condition, data was pooled across analyzed runs and blocks of the same condition within a run. ANOVA revealed no significant difference across the three visual stimulus conditions for any of these five eye movement parameters.

	PO		PL		PA	
	L	**R**	**L**	**R**	**L**	**R**
M1	5.6	7.8	0	5.9	0	5.9
M2	13.7	13.7	0	5.9	13.7	13.7
M3	17.6	23.4	15.6	39.1	0	0
M4	17.6	21.5	0	11.7	0	0
Mean	16.1	16.6	3.9	15.6	3.4	4.9
Std	1.6	6.2	6.8	13.7	5.9	5.6

Supplementary Table 1. The size (in mm^3) of the three macaque prefrontal face patches in left and right hemispheres of four macaques tested, at $p < 0.001$. Note that in monkey M3, we used a different MR sequence than in the other monkeys, which may account in part for the larger size of the patches in this monkey (see Supplementary Methods for details).

Patches of face-selective cortex in the macaque frontal lobe

Doris Y. Tsao, Nicole Schweers, Sebastian Moeller, Winrich A. Freiwald

Supplementary Methods

All animal procedures complied with the NIH Guide for Care and Use of Laboratory Animals, regulations for the welfare of experimental animals issued by the Federal Government of Germany, and stipulations of Bremen authorities.

Surgery. The implantation of the MR-compatible headpost (Ultem, General Electric Plastics) followed standard anesthetic, aseptic, and postoperative treatment protocols which have been described in detail elsewhere [1]. MR-compatible ceramic screws (Thomas Recording) and acrylic cement (Grip Cement, Caulk, Dentsply International) were used to secure the headpost to the skull.

Monkey fMRI. All scanning was performed in a 3T MR scanner (Allegra, Siemens). For each monkey we acquired 10 anatomical volumes at high spatial resolution (0.5 mm isometric). We used a T1 weighted inversion recovery sequence (MPRAGE). These scans were performed under anesthesia (Ketamin / Medetomidine, 8 mg/kg / 0.04 mg/kg) to reduce motion artifacts.

For all functional imaging, a contrast agent, ferumoxtran-10 (Sinerem, Guerbet, France; concentration: 21 mg Fe/ml in saline; dosage: 8 mg Fe/kg) was injected into the femoral vein prior to each scan session. Sinerem is the same compound as MION, produced under a different name [2]. Sinerem/MION increases signal-to-noise and gives finer spatial localization than BOLD [3-5]. Sinerem results in a signal reduction at activated voxels; for all functional data we inverted the signal to facilitate comparison with BOLD data.

All functional data was acquired in coronal slices. For data presented in Fig. 1a (M1, M2, and M4), we used a multi echo sequence (EPI, TR 4 s, TE 30 or 25 ms, 64 by 64 matrix). In combination with a concomitantly acquired fieldmap, this allowed high fidelity reconstruction by undistorting most of the B0-field inhomogeneities [6,7]. For data presented in Fig. 1a (M3) we used a standard single-shot EPI sequence (TR 2 s, TE 24 s,

64 by 64 matrix); this sequence generally produces larger activations because it does not correct for motion-induced distortions (the signal dropoff in the fieldmap due to the large muscles of monkey M3 prevented us from using the multi-echo sequence with undistortion as for the other three monkeys).

The data for each animal shown in Fig. 1 was acquired over two scan sessions (M1: 24 runs in 2 sessions, M2: 23 runs in 2 sessions, M3: 17 runs in 2 sessions, M4: 27 runs in 2 sessions). In these localizer experiments we acquired 136 volumes per run (28 slices, spatial resolution 1.25 mm isometric). The slice volume was adjusted for each monkey to cover the entire frontal lobe. The data for Fig. 2 was acquired over one scan session in monkeys M1 and M4 (M1: 12 runs, M4: 13 runs), and two scan sessions in monkey M3 (24 runs).

Visual stimulation. The face patch localizer stimulus followed a block design. Blocks lasted 32 seconds, and included the following image categories: human faces (F), monkey faces (M), human hands (H), gadgets (G), fruits and vegetables (V), and headless bodies (B). There were 16 different images in each category. Each image block was preceded by a block consisting of scrambled versions of the same images (S), resulting in the following sequence: S F S H S M S G S F S V S M S B R (the final block consisted of a gray random dot pattern). Each image subtended 12° visual angle (10.4 cm diameter at 49 cm distance), and was presented for 0.5 s.

The expression stimulus also followed a block design. Blocks lasted 32 seconds, and included the following image categories: neutral macaque faces (N), expressive macaque faces (E), and mixed non-face objects (O). There were 16 images in the two face categories, and 32 images in the object category. Each image block was preceded by a block of mean gray (G), resulting in the following sequence: G N G E G O G N G E G O G.

Visual stimulation was performed using custom code utilizing the Psychophysics Toolbox [8]. The stimuli were displayed at 60 Hz with a resolution of 1280 by 1024 pixels, using a video beamer (JVC DLA -G15E) and a back projection screen.

fMRI data analysis. We used FreeSurfer and FSFAST (http://surfer.nmr.mgh.harvard.edu) to reconstruct cortical surfaces and perform functional data analysis, following procedures detailed in [9]. To define face-selective areas we calculated the contrast faces versus all other objects (without scrambled images). Color scale bars show the significance of the contrast maps as negative common logarithm of the probability of error.

The stereotaxic coordinates of the slices were obtained as follows: each brain was rotated to align the anterior and posterior commissures. Then the slice most closely matching AP 0 in Red's Atlas [10] was assigned to AP 0.

A t-test was used to determine the significance of the difference in activation to expressive vs. neutral faces (Fig. 2c, Supplementary Fig. 2c), with voxels pooled across all monkeys for each patch. A two-way ANOVA with monkey identity and visual stimulus condition as factors was used to determine the significance of differences in the five eye movements parameters (horizontal eye position standard deviation, vertical eye position standard deviation, mean saccade frequency, mean saccade amplitude, and mean saccade duration) across visual stimulus conditions (Supplementary Fig. 3b).

Eye movement analysis. Blinks were removed from the eye trace prior to analysis. Saccades were detected by the methods described in [11]. The threshold for a saccade velocity was set to 20°/s to account for the reduced sampling frequency and increased noise level of our eye measurements compared to [11]. Saccade amplitude was computed by subtracting the end saccade position from initial saccade position. It was assumed that between saccades there was a linear slow drift. Supplementary Fig. 3b shows an example raw eye movement trace together with the fitted estimator, a straight line which only has breaks at saccade start and endpoints. Plots of peak velocity v versus movement amplitude d in log-log scale fell along the "main sequence" reported for primates [11-13]

(Supplementary Fig. 3c, left column), providing evidence that our saccade detection algorithm worked.

Supplementary Note: Assigning areas to prefrontal face patches

Macaque prefrontal cortex has been parceled into multiple subregions based on cytoarchitectonic and connectional data. Fig. 1f (top) shows a map of these areas, adapted from Petrides [14]. On the orbital surface, area 47/12 includes all of the cortex within the lateral orbital sulcus. PO lies in the lateral orbital sulcus, within area 47/12. PL was located close to the infraprincipal dimple. The anterior end of the infraprinciple dimple provides a useful landmark for the junction between areas 9/46v, 47/12, and 45A; PL could thus contain parts of any of these three areas. PA was located in the rostral bank of the inferior ramus of the arcuate sulcus, close to the border between areas 44 and 45B.

References

1. Wegener, D., Freiwald, W.A. & Kreiter, A.K. The influence of sustained selective attention on stimulus selectivity in macaque visual area MT. *J Neurosci* 24, 6106-14 (2004).
2. Nelissen, K., Luppino, G., Vanduffel, W., Rizzolatti, G. & Orban, G.A. Observing others: multiple action representation in the frontal lobe. *Science* 310, 332-6 (2005).
3. Leite, F.P. et al. Repeated fMRI using iron oxide contrast agent in awake, behaving macaques at 3 Tesla. *Neuroimage* 16, 283-94 (2002).
4. Vanduffel, W. et al. Visual motion processing investigated using contrast agent-enhanced fMRI in awake behaving monkeys. *Neuron* 32, 565-77 (2001).
5. Zhao, F., Wang, P., Hendrich, K., Ugurbil, K. & Kim, S.G. Coritcal layer-dependent BOLD and CBV responses measured by spin-echo and gradient-echo fMRI: Insights into hemidynamic regulation. *Neuroimage* 30, 1149 (2006).
6. Cusack, R., Brett, M. & Osswald, K. An evaluation of the use of magnetic field maps to undistort echo-planar images. *Neuroimage* 18, 127-42 (2003).
7. Zeng, H. & Constable, R.T. Image distortion correction in EPI: comparison of field mapping with point spread function mapping. *Magn Reson Med* 48, 137-46 (2002).
8. Brainard, D.H. The Psychophysics Toolbox. *Spat Vis* 10, 433-6 (1997).
9. Tsao, D.Y., Freiwald, W.A., Knutsen, T.A., Mandeville, J.B. & Tootell, R.B. Faces and objects in macaque cerebral cortex. *Nat Neurosci* 6, 989-95 (2003).
10. Ungerleider, L.G. *Red's atlas*, (Laboratory of Neuropsychology, NIMH Department of Health and Human Services.).
11. Bair, W. & O'Keefe, L.P. The influence of fixational eye movements on the response of neurons in area MT of the macaque. *Vis Neurosci* 15, 779-86 (1998).
12. Bahill, A.T., Clark, M.R. & Stark, L. The main sequence, a tool for studying human eye movements. *Mathematical Biosciences* 24, 191-204 (1975).

13. Mitchell, J.F., Sundberg, K.A. & Reynolds, J.H. Differential attention-dependent response modulation across cell classes in macaque visual area V4. *Neuron* 55, 131-41 (2007).
14. Petrides, M. Lateral prefrontal cortex: architectonic and functional organization. *Philos Trans R Soc Lond B Biol Sci* 360, 781-95 (2005).